Journal of Alloys and Compounds 489 (2010) 576–581

Contents lists available at ScienceDirect

Journal of Alloys and Compounds

journal homepage: www.elsevier.com/locate/jallcom

$La_{0.6}Sr_{0.4}Co_{0.2}Fe_{0.8}O_3$ protective coatings for solid oxide fuel cell interconnect deposited by screen printing

Ming-Jui Tsai, Chun-Lin Chu*, Shyong Lee

Department of Mechanical Engineering, National Central University, Chung-li, Taiwan

ARTICLE INFO

Article history:
Received 9 March 2009
Received in revised form
21 September 2009
Accepted 22 September 2009
Available online 25 September 2009

Keywords:
Solid oxide fuel cell (SOFC)
Interconnect
Screen printing

ABSTRACT

$La_{0.6}Sr_{0.4}Co_{0.2}Fe_{0.8}O_3$ (LSCF) is applied on a Crofer22 APU interconnect for solid oxide fuel cells (SOFCs) by screen-printing method. The above coated alloy was first checked for their compositions, morphology and interface conditions. It was then tested in a simulated oxidizing environment, 800 °C for 200 h. The results showed that the LSCF film can change the oxidation behavior of Crofer22 APU. After sintering the screen printed alloy was under 1050 °C in N_2 atmosphere, the adhesion between the LSCF layer and alloy substrate is excellent. Long-term electrical resistance measurement indicated that area-specific resistance (ASR) of the alloy with coated film is significantly lower than that of the uncoated. The use of LSCF coating for metallic interconnect could reduce working temperature for solid oxide fuel cell.

Published by Elsevier B.V.

1. Introduction

Solid oxide fuel cell (SOFC) is highly promising to warrant significant attention due to its high efficiency, fuel flexibility and environmental advantages. It directly converts the chemical energy of fossil fuels into electricity without combustion and mechanical processes. It has attracted significant attention due to its high efficiency, fuel flexibility and environmental advantages. The interconnect is a critical component of SOFC stacks, especially for the planar design, which physically separates the oxidant and fuel gases, distributes the gases to electrodes and provides electrical connection between adjacent cells. Because of the relatively high operating temperature, the requirements for interconnect materials are quite stringent, such as high-temperature oxidation resistance in both anode and cathode atmospheres, high electrical conductivity, thermal expansion compatibility with other cell components. Recent progresses in reducing SOFC operation temperature from 1000 °C to an intermediate temperature of about 600–800 °C allow the use of oxidation resistant metallic alloys as interconnect materials with advantages of easy fabrication, low material cost, significantly better mechanical properties and higher electric and thermal conductivity [1–4]. Alloys of high-temperature oxidation resistance used as interconnect in SOFC generally contain chromium as an alloying element to form a protective chromium oxide scale (Cr_2O_3). At high temperatures volatile Cr species such as CrO_3 and $Cr(OH)_2O_2$ are generated over the oxide scale in oxidizing atmospheres [5–8]. This substance will poison the interface between cathode and electrolyte. Thus, the performance of SOFC will decline rapidly. For this reason, it needs to coat a protective layer on SOFC interconnect in order to increase the anti-oxidative ability of stainless steel. Thereby it will extend the life-time of SOFC. Surface modifications, like protective coatings, are inevitably required to promote oxidation resistance and depress Cr vaporization in the long run [9–13]. LSCF is probably one of the most common materials used as cathodes for O_2 reduction reactions in SOFC. LSCF is a good electronic conductor, has high stability with electrolyte and high electrochemical activity for the O_2 reduction at high temperatures. It has been shown that LSCF material displays minimal reaction toward methane oxidation, while exhibiting resistance to carbon deposition [14–16]. The materials for anode and cathode often bear compositions similar to that of LSCF. So, using LSCF to coat interconnect would be desirable considering thermal expansion and chemical compatibility. In this work, the major concerns regarding these metallic interconnect are to investigate protective ceramic layer coating technology with stable electric conductivity by screen-printing process. The Crofer22 APU was selected as metallic material and alloy was coated with LSCF film, followed by oxidation at 800 °C for 200 h in hot air environment. Their compositions, morphology and interface conditions are then checked and analyzed to determine whether the oxidation behavior of their base alloy, Crofer22 APU, is changed in the presence of LSCF coating. Electrical resistance will be measured at elevated temperature to determine how effective the LSM film is when coated on the presently

* Corresponding author. Tel.: +886 3 4267 377; fax: +886 3 4254 501.
E-mail address: jenlen.boy@msa.hinet.net (C.-L. Chu).

0925-8388/$ – see front matter. Published by Elsevier B.V.
doi:10.1016/j.jallcom.2009.09.114

Table 1
Chemical compositions of the alloys (wt.%).

Alloys	Fe	Ni	Cr	Mn	Si	Mo	V	Cu	Ti	Al	Nb	C	RE
Crofer22 APU	Bal.	0.02	22.57	0.47	0.03	0.01	0.02	0.01	0.06	–	0.01	0.01	0.06La

best available metallic interconnect materials. The LSCF coated on Crofer22 APU alloy, containing comparable amount of Cr were subjected to oxidation treatment in hot air environment (simulating the SOFC cathode atmosphere) for various period of time, by using the oxide scale electron probe micro-analyzer (EPMA), high resolution transmission electron microscope (HRTEM), scanning electron microscope (SEM) and X-ray diffraction, verifying the applicability of the LSCF-coated alloys for the SOFC interconnect component.

2. Experimental

One type of metallic material, Crofer22 APU is used as the base of coating of LSCF. Their compositions as determined by induction coupled plasma (ICP)-AES and Spark-OES instruments are listed in Table 1. The preparation of LSCF paste for coating film by applying screen printing starts with mixing four kinds of high purity (99.9%) oxide powder, La_2O_3, $SrCO_3$, Fe_2O_3 and Co_3O_4 at a specific ratio. They are first poured into a container and wetted with alcohol, then stirred and ground for 24 h with a ball-type grinding apparatus to obtain a presumably homogeneous mixture. Subsequently, the mixed powder is dried in an oven to evaporate the alcohol, and taken out to pass a screener of 325 mesh. This particle-size controlled mixture is calcined at 1200 °C for 2 h to obtain LSCF powder which is then added with 1 wt.% bonding reagent – PVB (Polyvinyl Butyral), and ground for 5 h to produce the paste. After calcination of laborious intermediate steps as described, the resulting final paste for painting is the $La_{0.6}Sr_{0.4}Co_{0.8}Fe_{0.2}O_3$ compound in particle form of ~60 nm (Fig. 1). The atomically resolved HRTEM image for the particle of interest reveals a highly crystalline plane with a few stacking faults. The distance between adjacent fringes is approximately 0.35 nm, which is similar to the *d*-spacing of the standard, $La_{0.6}Sr_{0.4}Co_{0.8}Fe_{0.2}O_3$. Now the LSCF is ready to be printed on the base alloys using a screen plate with the designed pattern. Before printing coating, the samples were cut to 10 mm × 10 mm × 2 mm. Each sample was then polished with sandpaper of grade 1200, washed under ultrasonic waves in three cleaning liquids (alcohol, acetone, and distilled water), and blown dry for later use. Finally, the printed specimen receives sintering treatment – 1100 °C for 50 min in 90%Ar + 10% vol.% N_2 atmospheric environment. This powder mass was melted in a heated electric furnace according to the program in Fig. 2. The material is thus termed a LSCF. After the above preparation, specimens were ready for the simulated oxidation test – 800 °C for 200 h. The oxide scale was observed and analyzed in surface and cross-sectional directions with a scanning microscope and other auxiliary apparatus. The coating completed surfaces via screen-printing method before oxidation tests are displayed in Fig. 3. The area-specific resistance (ASR) of the Fe–Cr alloys was measured as a function of holding time and temperature in air by using a two-point, four-wire probe. For determining the electrical resistance of the oxide scale, two surfaces of the oxidized coupon were covered with Pt paste, and Pt meshes attached with four Pt leads were placed on top of the paste for applying current and voltage measurement, as schematically shown in Fig. 4. The procedure for measuring ASR is to follow the most common one as referring literatures [17,18]. The ASR of the oxidized coupon, which reflects both the electrical conductivity and thickness of the oxide scale, was calculated according to Ohm's Law, $R = V/I$ and the ASR = $1/2\,R \times S$, where V is the voltage drop, I is the constant current, R is the resistance, S is the area covered by Ag paste, and the factor

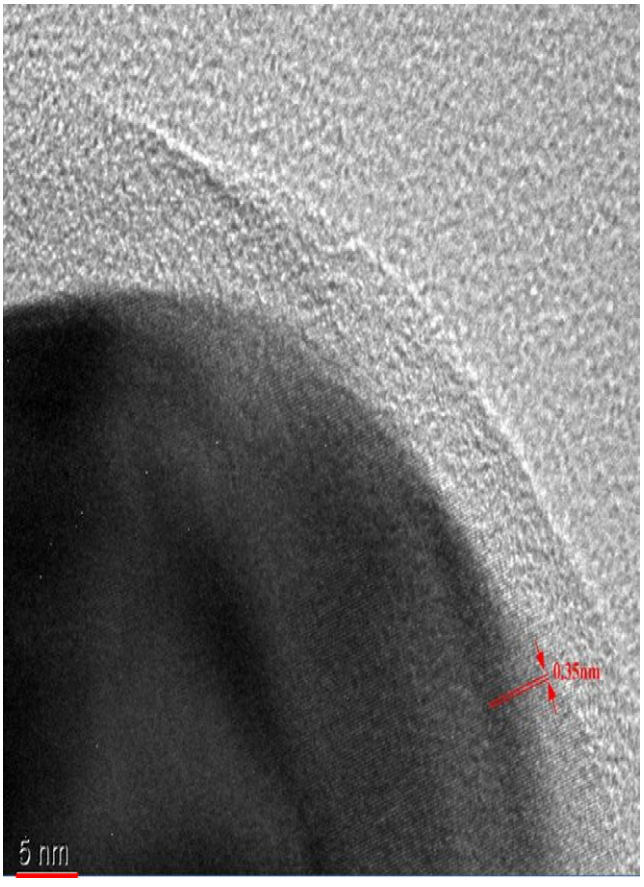

Fig. 1. Atomically resolved HRTEM image of LSCF powder calcined at 1200 °C for 2 h.

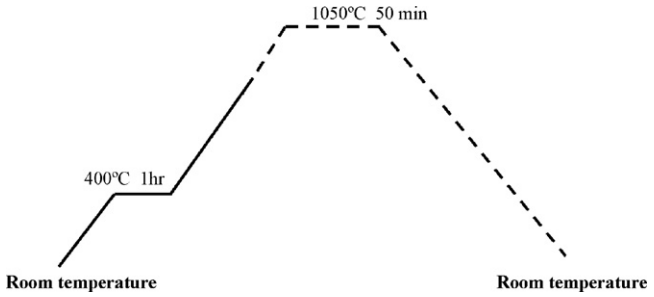

Fig. 2. Schedule followed for the melting of LSCF.

Fig. 3. Surfaces appearances of screen printed coating before oxidation test.

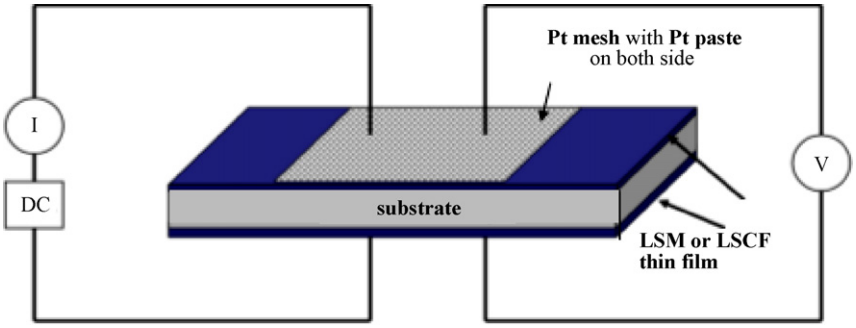

Fig. 4. Apparatus for measuring area-specific resistance.

1/2 is used to represent the contribution of the oxide scale on one surface to the ASR.

3. Results and discussion

3.1. Oxidized surface microstructure analysis by XRD and SEM

Fig. 5 displays the X-ray diffraction (XRD) patterns of LSCF powders. The XRD patterns reveal the perovskite structure, and in particular formation of a single perovskite phase in the LSCF powders. Fig. 5(a) indicates that the XRD patterns of the powder are formed by the heating of a perovskite structure at 1100 °C for 50 min in hot air. The XRD patterns show that a crystalline structure was formed. Fig. 5(b) presents the samples that were oxidized at 800 °C for 200 h. Fig. 5 clearly indicates that the oxides were composed of $CoFe_2O_4$ spinel in the sample, indicating that coating with a reactive element change the structure of the LSCF from a loose phase structures to a compact ones, markedly improving the high-temperature oxidation resistance of the samples. Fig. 6 presents

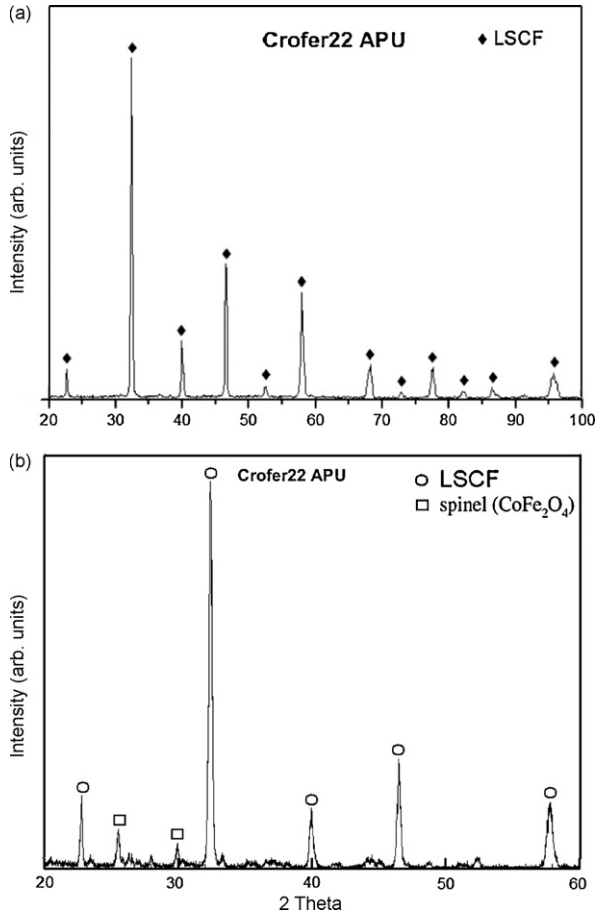

Fig. 5. XRD pattern of a LSCF film deposited on substrate. (a) Sintering at 1050 °C for 50 min, (b) oxidized surface as processed at 800 °C for 200 h.

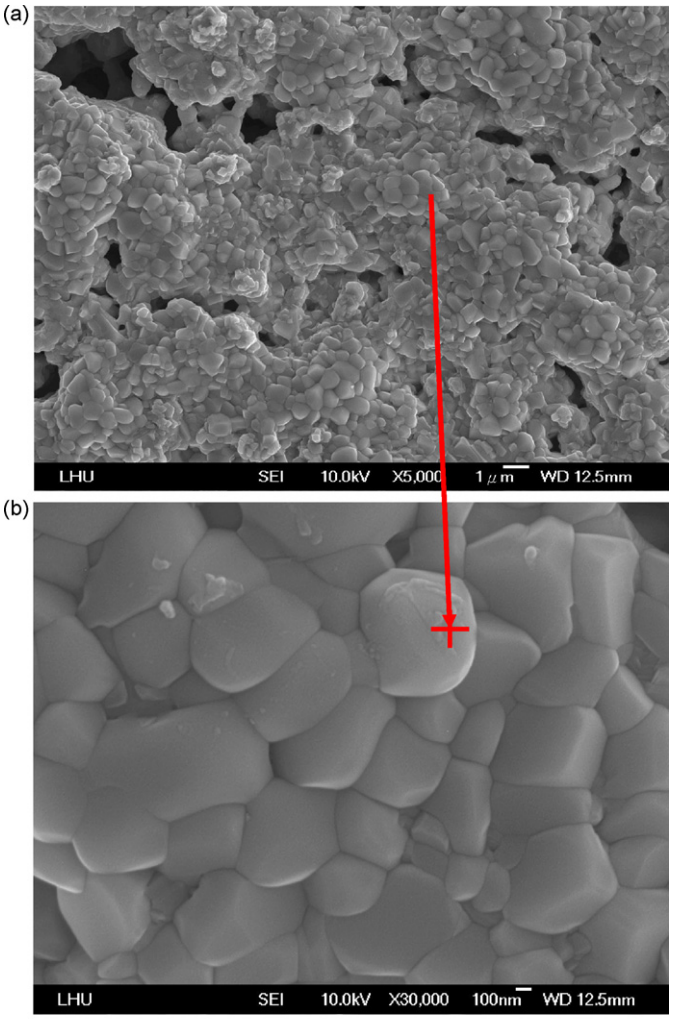

Element	O	Co	La	Sr	Fe
at%	65.56	4.3	9.56	10.27	10.31

Fig. 6. Micrographs of the oxidized (in 800 °C hot air) surfaces of LSCF/Crofer22 APU displaying small granular portions, (b) enlarged micrographs with EDS.

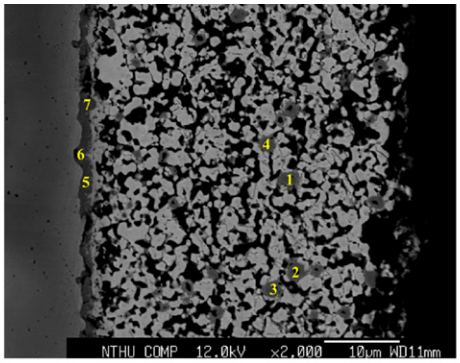

Element / at%	Sr	La	O	Mn	Co	Cr	Fe
1	0.05	0.25	57.11	-------	39.49	0.09	3.00
2	0.07	0.34	60.15	-------	36.24	0.11	3.09
3	0.07	0.29	61.36	-------	35.17	0.09	3.00
4	0.08	0.26	59.10	0.02	37.68	0.04	2.84
5	0.25	0.15	60.39	10.11	3.50	23.94	1.66
6	0.37	0.15	60.46	11.40	3.55	21.66	2.41
7	0.31	0.12	59.05	9.12	3.58	26.37	1.44

Fig. 7. Micrographs of oxide scale/alloy interface of LSCF-coated Crofer22 APU and corresponding EDS quantitative analysis after 800 °C for 200 h by screen painting.

SEM micrographs of the surface of Crofer22 APU/LSCF after they were annealed at 800 °C for 200 h. Nano-sized particles with diameters of between 200 and 500 nm were observed on the surface of the LSCF structure. The size of the LSCF particles was reduced probably because of its low coarsening and sintering temperatures (1000 °C for 50 min). As the oxidation time passed, the quantity of the LSCF gradually increased, and some fine particles filled, forming a continuous and porous Crofer22 APU/LSCF network. A close-up micrograph (Fig. 6(b)) reveals a perovskite structure. Since the SEM/EDS analysis reveals a significant oxygen content, each grains contains an oxide compound. The surface is decorated by a densely compacted prism-like oxide, cubic-structured spinel, which grew and became increasingly compact with oxidation time.

3.2. Microstructural analysis and discussion of the results

Fig. 7 shows secondary electron micrographs and the results of an EDS quantitative analysis of the fractured surface after oxidation at 800 °C for 200 h. The figure shows the proportion of Fe, La, Sr, Co, O, Cr and Mn (at.%) at various points. The values of oxide scale at position (5)–(7) show that the surface is completely covered with small crystals that comprise mostly Cr_2O_3 with some $MnCr_2O_4$ and $FeCr_2O_4$. At these three positions (5)–(7) oxide scale was detected in the alloy because the scale was thin, with a thickness of 1 μm. In the alloy, other four positions (1)–(4) were also detected because these are very close to the scale/alloy boundary. The values of oxide scale at (1)–(4) show that the crystals that appeared on the surface of the scale were LSCF. The LSCF scale was composed of LSCF and $CoFe_2O_4$. At four points (1)–(4), Mn and Cr were barely detected on the surface of the scale, revealing alloy grain boundaries, indicating that the conditions of sintering following LSCF coating are important to forming a stable coating layer and an interfacial oxide layer. Fig. 8 presents the BEI (backscatter electron image) and EPMA (electron probe micro-analysis) of Crofer22 APU/LSCF by screen printing. Small particles were not bounded and many small pores were present in the coating layer. However, the densification characteristics of the coating materials directly determine the density of the coating layers, and therefore, the effectiveness of the chromium vaporization barrier. The EPMA analysis suggests that the dense layer contains Cr_2O_3 or $CoFe_2O_4$ spinel phase, which is comprised of Fe, Cr, La, Sr, Mn, Co and O. The innermost layer has the Fe–Cr matrix phase. The continuous $CoFe_2O_4$ spinel layer on the surface of Crofer22 APU significantly reduces vaporization of chromium.

3.3. Electrical resistance

Fig. 9 plots the ASR parameter of oxidized Crofer22 APU at 800 °C for 300 h by screen printing. The slop in Fig. 9 is some-

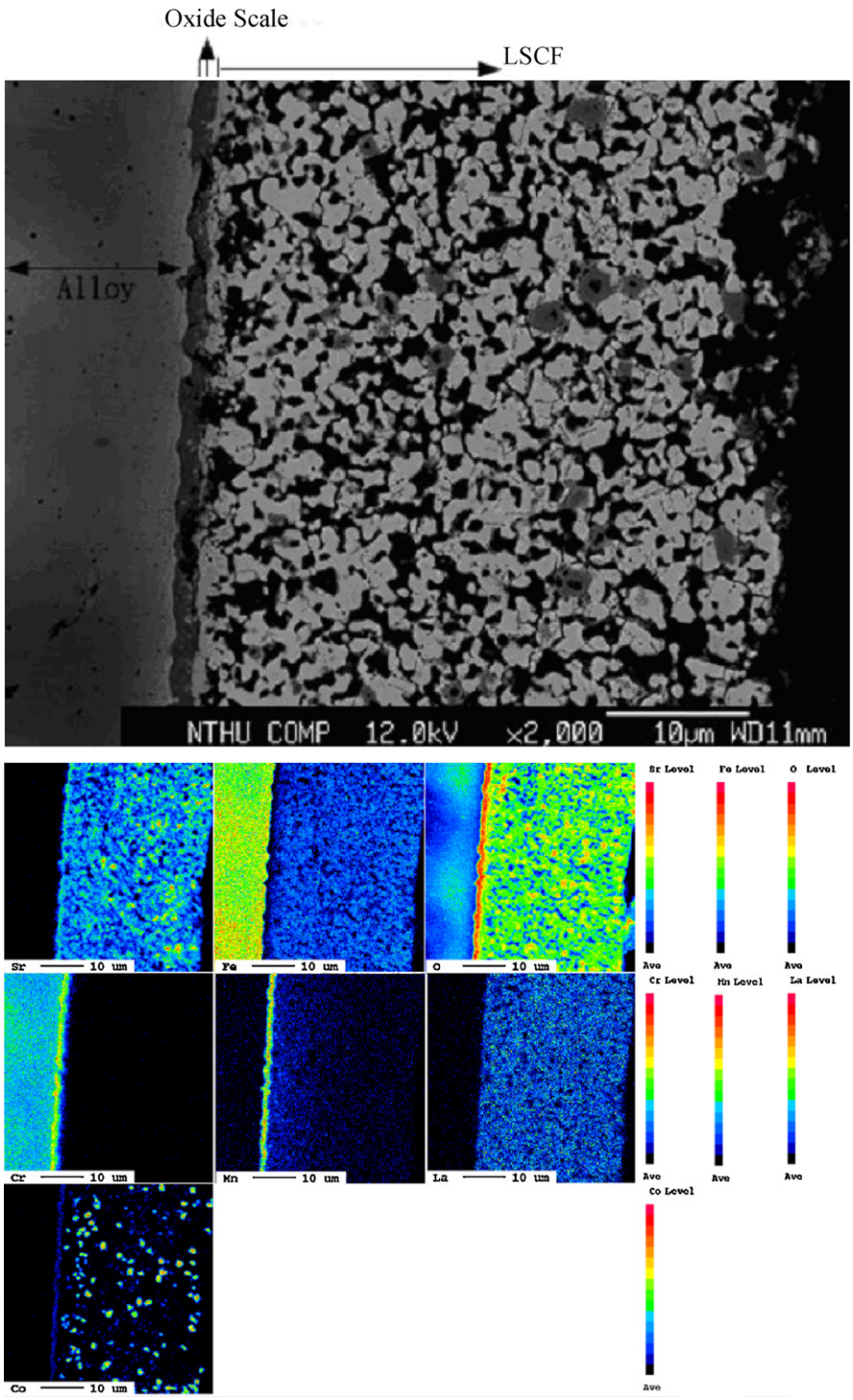

Fig. 8. Micrographs of oxide scale/alloy interface of LSCF-coated Crofer22 APU and corresponding EPMA indicates that compounds are of Cr, O, Fe, La, Sr and Co at 800 °C for 200 h by screen painting.

what reduced after about 300 h of LSCF-coating oxidation by screen printing; this process is a two-stage oxidation such that the ASR curve has two slopes. The slop rate constant in the first stage (0–40 h) is estimated to be 0.014 Ω cm^2, while that in the second stage (40–300 h) is 0.054 Ω cm^2. Accordingly, the change in the area-specific electrical resistance as a function of oxidation time is attributable an increase in the thickness in the oxide scale. The above-mentioned preliminary results show that the LSCF thin film that is coated on the Crofer22 APU can indeed retard the high-temperature oxidation of metal. This phenomenon should be related to the steady production of $CoFe_2O_4$ spinels.

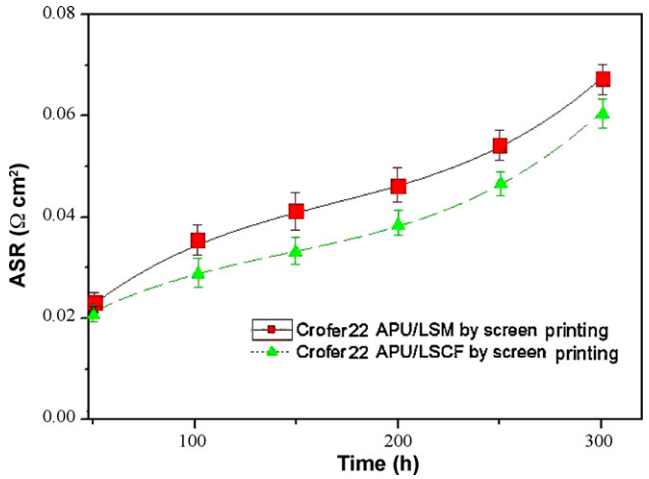

Fig. 9. Area-specific resistance of LSCF or LSM-coated alloys as a function of holding time 800 °C for 300 h in hot air.

4. Summary

Thick $La_{0.6}Sr_{0.4}Co_{0.8}Fe_{0.2}O_3$ film was deposited as a protective coating and candidate SOFC interconnect material by screen printing on Crofer22 APU. The alloy was coated by LSCF sintering at 1050 °C in an N_2 atmosphere, and the adhesion at the LSCF layer/alloy interface was excellent. After measurements of long-term electrical resistance were made, the ASR of alloy that was coated with LSCF was less than for an alloy that was coated with LSM. The use of LSCF as a metallic interconnect protective material could increase high-temperature conductivity. Accordingly, LSCF films, deposited by screen printing are good candidates for protective coatings of Crofer22 APU and can be used as an SOFC interconnects.

References

[1] N.Q. Minh, T. Takahashi, Science and Technology of Ceramic Fuel Cell, Elsevier Science, 1995.
[2] W.Z. Zhu, S.C. Deevi, Mater. Sci. Eng. A 348 (2003) 227.
[3] J.W. Fergus, Mater. Sci. Eng. A 397 (2005) 271.
[4] Z. Yang, Int. Mater. Rev. 53 (2008) 39.
[5] Z. Yang, K.S. Weil, D.M. Paxton, J.W. Stevenson, J. Electrochem. Soc. 150 (2003) A1188.
[6] S.P. Jiang, S. Zhang, Y.D. Zhen, J. Mater. Res. 20 (2005) 747.
[7] J.W. Fergus, Int. J. Hydrogen Energy 32 (2007) 3664.
[8] E. Konysheva, H. Penkalla, E. Wessel, J. Mertens, U. Seeling, L. Singheiser, K. Hilpert, J. Electrochem. Soc. 153 (2006) A765.
[9] W. Qu, J. Li, D.G. Ivey, J. Power Sources 138 (2004) 162.
[10] Z. Yang, G. Xia, S.P. Simner, J.W. Stevenson, J. Electrochem. A1896 (2005).
[11] P. Piccardo, P. Gannon, S. Chevalier, M. Viviani, A. Barbucci, G. Caboche, Amendola, S. Fontana, Surf. Coat. Technol. 202 (2007) 1221.
[12] H. Kurokawa, C.P. Jacobson, L.C. DeJonghe, S.J. Visco, Solid State 178 (2007) 287.
[13] C. Chu, J. Wang, S. Lee, Int. J. Hydrogen Energy 33 (2008) 2536.
[14] C. Jin, J. Liu, W. Guo, Y. Zhang, J. Power Sources 183 (2008) 506.
[15] J. Liu, A.C. Co, S. Paulson, V.I. Birss, Solid State Ionics 177 (2006) 377.
[16] S.P. Jiang, Solid State Ionics 146 (2002) 1.
[17] W.Z. Zhu, S.C. Deevi, Mater. Res. Bull. 38 (6) (2003) 957.
[18] J.H. Kim, R.H. Song, S.H. Hyun, Solid State Ionics 174 (2004) 185.